The surface electronic structure of (1*1) Pt(001)

1990 J. Phys.: Condens. Matter 2 9065

(http://iopscience.iop.org/0953-8984/2/46/007)

J. Phys.: Condens. Matter 2 (1990) 9065–9076. Printed in the UK

The surface electronic structure of (1 × 1) Pt(001)

G A Benesh†‡, L S G Liyanage†‡ and J C Pingel†
† Department of Physics, Baylor University, Waco, Texas 76798, USA
‡ Cavendish Laboratory, Madingley Road, Cambridge CB3 0HE, UK

Received 14 May 1990

Abstract. We have performed first-principles calculations of the electronic structure of the unreconstructed metastable (1 × 1) Pt(001) surface using the surface embedded Green function (SEGF) method for a semi-infinite geometry. Our calculated work function of 5.9 eV is in excellent agreement with experiment. Calculated surface state and surface resonance bands are compared with those found in angle-resolved photoemission experiments and earlier slab calculations. Analysis of the charge density at the surface shows an increase in sp bonding charge which leads to a surface tension similar to that found on Au(001), and may help explain the (5 × 20) reconstruction.

1. Introduction

The industrial use of platinum in heterogeneous catalysis has encouraged much experimental study of the low index faces. Experiment has revealed that chemical activities of important adsorbates often vary markedly according to the geometry of the Pt surface exposed. For example, the sticking coefficients of molecularly adsorbed oxygen and hydrogen are three orders of magnitude greater for the clean, unreconstructed (1 × 1) phase of Pt(001) than for the (5 × 20) reconstructed phase [1]. The heat of adsorption of CO on Pt surfaces has been shown to vary as: Pt(001)(1 × 1) > Pt(111) > Pt(001)(5 × 20) > Pt(110) [2, 3]. Several important catalytic reactions on Pt surfaces have also exhibited a crystal face-dependent activity. Somorjai and co-workers have shown that the production rate of benzene and toluene by the dehydro-cyclization of n-hexane and n-heptane is greater for Pt(111) than for either Pt(001) or Pt(110) [4]. In contrast, the isomerization rate of isobutane into methane, ethane, propane and n-butane is higher for Pt(001) than for Pt(111) [4]. The decomposition or dissociation of small inorganic molecules also shows evidence of face-dependent activity [5, 6]. An extensively studied example is the dissociation of NO on Pt which varies as: Pt(410) ≫ Pt(210) > Pt(100)(1 × 1) ≫ Pt(110), Pt(111) [7].

Why does a single crystal show such a range of chemical activity depending on the surface exposed? The bulk states, while important to the chemical bonding at the surface, cannot explain the difference in behaviour—since the same spectrum of bulk wavefunctions are present at each of a crystal's surfaces. It must be the unique features in a surface's electronic structure (the surface state and surface resonance bands) together with the molecular levels of the adsorbed species which determine the difference in behaviour. A detailed investigation is therefore important to determine how the particular electronic features present determine a surface's chemical activity.

0953-8984/90/469065 + 12 $03.50

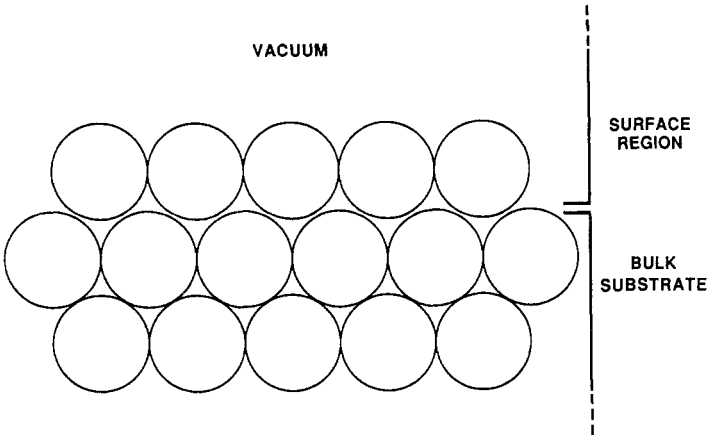

Figure 1. Semi-infinite crystal surface as modelled by the SEGF method. Surface atomic layers are embedded on to the bulk substrate.

We have performed a self-consistent Surface Embedding Green Function (SEGF) calculation for a Pt(001) slab embedded on to the bulk platinum crystal—resulting in a semi-infinite geometry for the surface. We have been motivated, in part, by angle-resolved photoemission experiments on the metastable (1 × 1) surface [8], which now allow a comparison to be made between theoretical and experimental surface bands. Our goal is to understand aspects of the face-dependence of chemical reactivity by accurately determining the surface state/surface resonance bands for a number of crystal faces. In addition, we wish to identify any changes in bonding character at the surface which might lead to the well-known (5 × 20) reconstruction of Pt(001) [9].

2. Computational aspects

The SEGF method [10, 11] has been used to calculate the electronic structure of the clean, unreconstructed Pt(001) surface. This method models the surface as a semi-infinite crystal with only one surface. The semi-infinite crystal surface is divided into two regions: the surface region and a bulk substrate (see figure 1). The surface region is defined as a thin film, or slab, consisting of a few atomic layers. The substrate region is taken as the perfect bulk crystal, truncated at the interface between the two regions. Thus, the substrate wavefunctions, including those with imaginary wavevector, are known. The wavefunctions in the surface region are calculated self-consistently subject to the boundary condition that they match onto the bulk wavefunctions along the interface. This is accomplished by including in the Hamiltonian an *embedding potential* obtained from the substrate Green function. As a result, information about the continua of bulk states is conveyed to the surface wavefunctions. Since only one surface is present, no splitting of surface state bands is artificially induced as in slab-only and supercell methods. Furthermore, the thickness of the surface region unit cell need only be one or two layers thick; thus, the computational problem is limited to the region of interest: the surface.

We have represented the clean, unreconstructed Pt(001) surface by a single layer of atoms embedded onto the bulk substrate. The surface lattice contains no relaxations

with respect to the perfect fcc bulk substrate. The embedding potential is derived from Weinert's self-consistent platinum potential [12], having a lattice parameter of 7.416 au. A total of 80 LAPW basis functions were used. Both the potential and charge density were taken to self-consistency without making any shape approximation in the surface region (as in the full-potential LAPW method). For exchange–correlation the Hedin–Lundqvist potential was used [13]. In each cycle the valence wavefunctions were calculated scalar-relativistically, and the core electrons fully relativistically. (The effect of omitting the spin–orbit interaction for the valence electrons is discussed below.) The valence charge density was then accumulated from the bottom of the bulk valence band up to the Fermi level. The charge was sampled over fifteen special $\boldsymbol{K}$-points in the irreducible wedge of the 2D Brillouin zone [14]. The surface region potential was considered to be self-consistent when the maximum difference between input and output was below 0.0032 au (0.09 eV).

3. Results

3.1. Work function and total charge density

Difficulties in acquiring an unreconstructed Pt(001) surface sufficiently free of adatoms have hampered efforts to obtain a reproducible value of the work function for clean unreconstructed Pt(001). Bonzel and Fisher measured the (5 × 20) reconstructed Pt(001) work function as 5.7 ± 0.1 eV [1]. Behm *et al* found that the work function for the unreconstructed surface was about 0.160 eV higher than that of the reconstructed surface [3]. In an extensive review of experimental studies of Pt(001) surfaces, Mundschau and Vanselow found that most earlier work did not have enough evidence to confirm that the studied surfaces were clean [15]. More recently, Drube *et al* have obtained an experimental work function of 5.9 eV for the (1 × 1) Pt(001) surface [16].

Two five-layer LAPW slab calculations of clean, unreconstructed Pt(001) have previously been performed. Wang *et al* [17] obtained a work function of 6.6 eV, while Weinert and Freeman [18] reported a value of 6.2 eV. (The improved value was obtained using the full-potential LAPW method.)

Using only a single surface layer embedded onto bulk platinum, our self-consistent potential yields a work function of 5.92 ± 0.09 eV, in excellent agreement with experiment. (Such accuracy for one and two embedded layers was earlier obtained for Al(001), where the long decay length of free electron-like surface states require much thicker slabs for comparable accuracy [19, 20]. Since the SEGF method correctly embeds the surface layer onto the bulk substrate, it is not surprising that accurate work functions may be obtained using fewer atomic layers.

The total charge density, which is calculated from the self-consistent potential in this study, is shown in figure 2. The charge density contours as calculated in this study are very similar to those of both five-layer slab calculations [17, 18]. As noted in the slab calculations, the healing length of the charge density is very short, so that only the top one or two surface layers differ from the bulk atomic layers. It also should be noted that the second Pt layer in figure 2 is not explicitly represented in the embedded slab. It enters the calculation implicitly through the embedding potential. However, the boundary condition on the surface wavefunctions—that they match on to bulk solutions of the Schrödinger equation across the embedding surface—causes the *valence* charge density

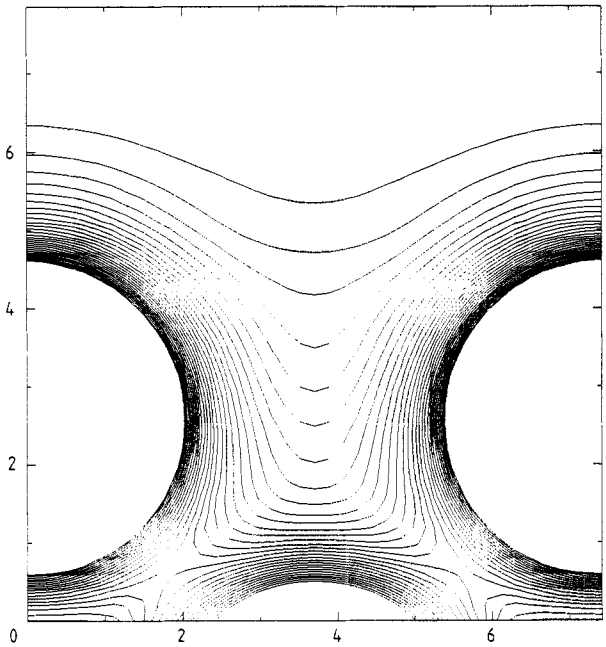

Figure 2. Self-consistent total charge density of the Pt(001) surface layer. Vacuum is at the top in the figure. The minimum contour is 0.003 electrons/a_0^3 and successive contours differ by 0.003 electrons/a_0^3.

to be accurate into the second layer. (The *core* charge density in the second layer is not included in the plot.)

3.2. *Surface state/surface resonance bands*

The surface density of states (DOS) at each wave vector $\boldsymbol{K}$ can be directly obtained from the surface Green function. The symmetry of each surface peak may then be found by decomposing the DOS or by plotting the charge density in the plane of the surface. The origin of the surface peaks may be understood from an analysis of the bulk bands which project into the particular value of $\boldsymbol{K}$.

In figure 3 we display the projected bulk band structure (PBS) for the Pt(001) (1×1) surface, as obtained from the bulk Green function. Both even- and odd-symmetry states along high symmetry lines are shown. Note that because the bulk states projecting into $\bar{Y}$ have no non-trivial symmetry, the same bands and band gaps exist for $\bar{Y}_1$ and $\bar{Y}_2$ states. Our PBS is very similar to that computed for Ir(001) by Bisi *et al* [21]. Differences, such as the ordering of bands near E_F at $\bar{X}$, may be attributed to relativistic corrections included in our calculation. Nevertheless, the differences are minor. The occupied bandwidth of 10.3 eV is in excellent agreement with that of relativistic bandstructure calculations [22] and represents an improvement over the 9.7 eV obtained in slab methods [17]. The influence of these bulk bands on the surface electronic structure is included explicitly in our surface calculation via the embedding potential. Thus, the PBS may be used to determine which surface peaks are truly surface states and which are surface resonances. (A drawback of supercell and other slab methods is that the

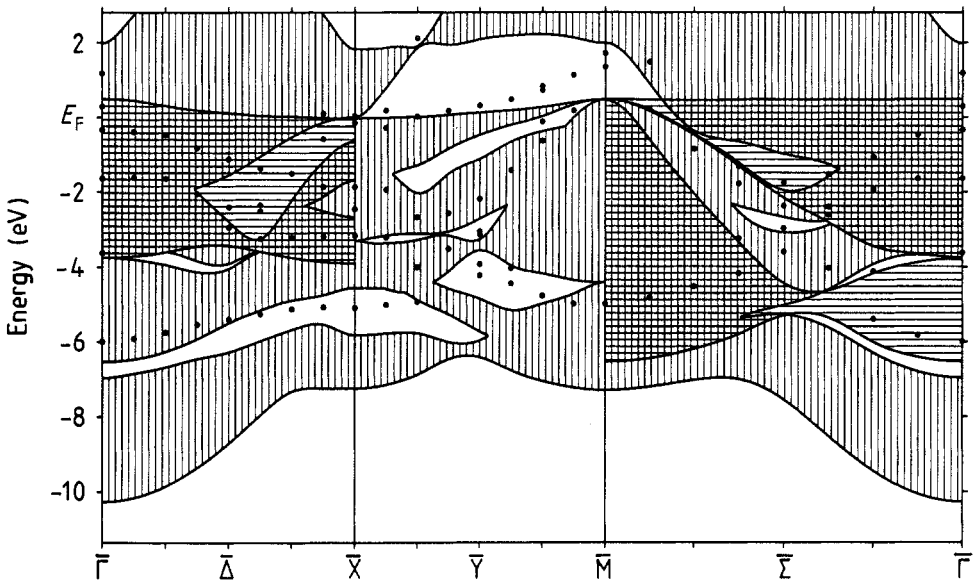

Figure 3. Pt(001) projected bulk band structure and SS/SR bands along the principal symmetry directions. Regions with vertical lines represent projected $\bar{\Delta}_1$, $\bar{Y}_1$, $\bar{Y}_2$ and $\bar{\Sigma}_1$ bulk bands; those with horizontal lines represent projected Δ_2 and $\bar{\Sigma}_2$ bulk bands. Dots mark surface states and surface resonances.

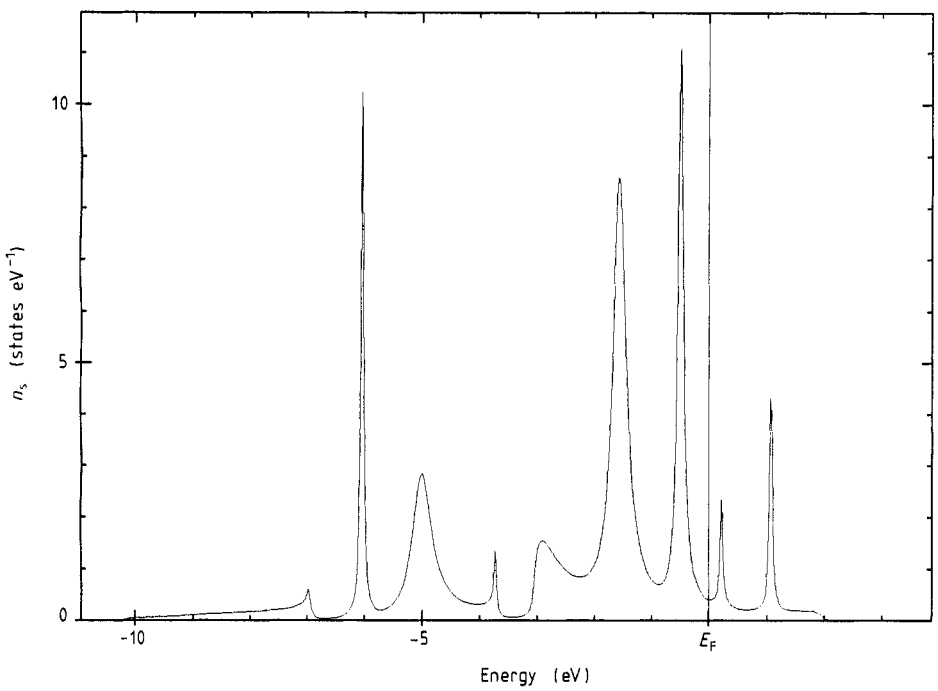

Figure 4. Pt(001) surface density of states at $\bar{\Gamma}$. Imaginary part of the energy = 0.001 au.

identification of surface states must be somewhat arbitrarily defined since bulk bands are absent from the calculation.)

Angle-resolved photoemission experiments for both the (5 × 20) and metastable (1 × 1) Pt(001) surfaces have been carried out by Brooks and King [8]. The (1 × 1) surface was prepared using the method described by Pirug *et al* [23]. In brief, the (5 × 20) surface was saturated with NO to stabilize the (1 × 1) structure. Next, the crystal was heated to 470 K to dissociate the molecules. The nitrogen was removed by heating, and hydrogen was introduced to react with the oxygen. Once water and excess hydrogen were removed by careful heating, a metastable (1 × 1) Pt(001) surface remained.

Four surface features near $\bar{\Gamma}$ are evident in photoemission spectra. Near $E_F - 6.0$ eV a surface peak was found using He I and Ne I radiation. This $\bar{\Gamma}$ state is part of a surface state/surface resonance (SS/SR) band which disperses upward in energy along both $\bar{\Sigma}$ and $\bar{\Delta}$. Halfway along $\bar{\Sigma}$ it reaches a maximum energy of $E_F - 5.0$ eV and then disperses downward in energy to the zone boundary at $\bar{M}$. Along $\bar{\Delta}$ the band disperses upward in energy all the way to $\bar{X}$ where it has an energy of $E_F - 4.8$ eV.

A second experimental $\bar{\Gamma}$ peak was observed near $E_F - 4$ eV. It is part of a fairly flat SS/SR band which extends across the $\bar{\Sigma}$ and $\bar{\Delta}$ directions. Along $\bar{\Sigma}$ the experimental band disperses slightly downward in energy, reching a minimum of $E_F - 4.5$ eV about three-fourths of the way to $\bar{X}$. Along $\bar{\Delta}$, the experimental dispersion is even more gradual; the band reaches a minimum of $E_F - 4.3$ eV near $\bar{M}$.

The most prominent $\bar{\Gamma}$ experimental peak is located at $E_F - 1.5$ eV. The relevant SS/SR band disperses downward in energy along $\bar{\Sigma}$, reaching a minimum of $E_F - 2.5$ eV halfway to $\bar{M}$. It then disperses upward in energy toward E_F at the zone boundary. The band remains fairly flat to one-fourth of $\bar{\Delta}$, then bends sharply down to reach $E_F - 2.7$ eV two-thirds of the way across the zone. Over the remaining third of $\bar{\Delta}$ the band is again flat and terminates as an $\bar{X}$ state at $E_F - 2.9$ eV.

The highest occupied surface band is seen experimentally at $E_F - 0.3$ eV at normal emission, dispersing downward in energy to $E_F - 0.6$ eV at one-third $\bar{\Delta}$. The band then seems to flatten out and disperse on to $\bar{X}$ at $E_F - 0.5$ eV. Along $\bar{\Sigma}$ there is confusion as to how many bands are involved in this energy range. It appears that away from $\bar{\Gamma}$ the band disperses downward for at least one-eighth $\bar{\Sigma}$. From that point on there are at least two, and possibly three, bands observed. One disperses down in energy while the other varies between 0.4 and 0.7 eV below E_F.

Also plotted in figure 3 are the calculated SS/SR bands along principal symmetry directions. In figure 4 we plot our calculated surface region DOS at $\bar{\Gamma}$, in which a small imaginary part has been added to the energies to broaden the surface state (delta-function) peaks. The SS/SR peaks are clearly distinguished.

The lowest SS/SR band in figure 3 begins as a $\bar{\Gamma}$ state at $E_F - 6.0$ eV with Δ_1 character. It is in excellent agreement with the lowest SS/SR band observed experimentally. The $\bar{\Gamma}$ state is formed in the Δ_1 hybridization gap between s and $3z^2 - r^2$ bulk states and exhibits some bonding toward the substrate. It is the same type of Shockley surface state first predicted to exist on Cu(001) by Gurman and Pendry [24] and seen in Cu(001) [25], Ni(001) [26], Pd(001) [27], Ir(001) [21] and Pt(001) [17] slab calculations. Along $\bar{\Delta}$ this state has only $\bar{\Delta}_1$ symmetry, and may hybridize with the continua of bulk states belonging to the same irreducible representation. It merges into a surface resonance band which extends halfway to $\bar{X}$. At this point the band enters the $\bar{\Delta}_1$ bulk gap and becomes a surface state band extending to $\bar{X}$. Similarly, in their fourteen-layer Ir(001) calculation, Bisi *et al* [21] find the SS/SR band to be a resonance to halfway along $\bar{\Delta}$ and a surface state

band thereafter. In a 33-layer slab calculation for Cu(001), Sohn *et al* [25] found a similar SS/SR band which dispersed along the top of the $\bar{\Delta}_1$ gap for one-third of $\bar{\Delta}$, crossed the gap at about the midpoint of $\bar{\Delta}$, then persisted along the bottom of the gap to $\bar{X}$. The $\bar{X}_1$ state at $E_F - 5.1$ eV is primarily $d_{x^2-y^2}$ character (with respect to the surface axes).

Along Y the band persists as an even (Y_1) surface state to one-fourth of the way to $\bar{M}$, where it merges into the bulk continuum. From $\bar{\Gamma}$ along the $\bar{\Sigma}$ direction, the band disperses as a surface state in the even-symmetry hybridization gap. At three-eighths of the way to $\bar{M}$ the gap closes, and the band disappears. To this point the dispersion of the band agrees with that observed in photoemission. Closer to $\bar{M}$, however, the experimental peaks may correspond to a second Shockley SS/SR $\bar{\Sigma}_1$ band. This band has an energy of $E_F - 5.0$ eV at $\bar{M}$ and disperses upward in energy along both $\bar{\Sigma}$ and into the hybridization gap in the middle of $\bar{Y}$. It has been identified in the 33-layer Cu(001) calculation both as a surface resonance near $\bar{M}$, and as a surface state band in the gap [25]. Near $\bar{M}$ the band has d_{xy} character, and has been identified in both the 5-layer and 14-layer calculations [17, 21].

A small peak occurs in the $\bar{\Gamma}$ DOS at $E_F - 3.6$ eV. This state has Δ_2 symmetry ($\Delta_{2'}$ with respect to bulk axes) and consists mostly of $d_{x^2-y^2}$ character. It contributes to the bonding within the surface layer, but not between surface and substrate. The upward shift in potential at the surface pulls this state off the top of the $\Delta_{2'}$ bulk band, creating a Tamm surface state localized to the top layer of atoms. Away from $\bar{\Gamma}$, the symmetry is reduced, and the surface state merges into a SR band which hybridizes with even symmetry bulk states along $\bar{\Delta}$ and $\bar{\Sigma}$. It is likely that this state is the one seen in the five-layer slab calculation dispersing upward in energy from $E_F - 4.0$ eV to about $E_F - 2.9$ eV at $\bar{X}$ [17]. However, unlike the slab results, away from $\bar{\Gamma}$ our DOS peak rapidly diminishes in amplitude as the band disappears into the bulk continuum. The agreement with the experimental bands dispersing across the surface BZ near $E_F - 4$ eV is not good. However, when the spin–orbit term is included in the Hamiltonian a gap is opened up across a fairly constant energy range centered on $E_F - 4$ eV. It extends all along $\bar{\Delta}$, $\bar{Y}$ and $\bar{\Sigma}$—being pinched off only at $\bar{\Gamma}$. A surface state band in this gap on Au(001) has been discussed by Pick and Tomášek [28]. The corresponding band on Pt(001) is probably that observed along both $\bar{\Delta}$ and $\bar{\Sigma}$ in the angle-resolved photoemission data [8].

The third $\bar{\Gamma}$ peak, $E_F - 1.6$ eV, lies near the bulk Γ_{12} eigenvalue where the bulk Δ_1 and Δ_2 bands are degenerate. As at other upper band edges, such as $E_F - 7.0$ eV and $E_F + 1.9$ eV, the upward shift in potential at the surface increases the energies of bulk-like states near the surface and creates a peak in the DOS. In addition to the band edges present, the Δ_5 bulk band, consisting largely of $d_{xz,yz}$ states, spans the energy range at higher $k_\perp$ wavevector. The surface resonance band extends one-fourth of the way along both $\bar{\Delta}$ and $\bar{\Sigma}$, diminishing as the Γ_{12} degeneracy is lifted. Closer to $\bar{X}$ a flat surface resonance band of $\bar{\Delta}_1$ character exists near $E_F - 3.2$ eV. At $\bar{X}$ the SR is largely d_{z^2} in character. Two $\bar{\Sigma}_2$ surface state bands can be identified in the large odd-symmetry hybridization gap along $\bar{\Sigma}$. The lower energy band is located in the middle third of $\bar{\Sigma}$ near $E_F - 3.9$ eV. The higher band begins at the centre of $\bar{\Sigma}$ at $E_F - 2.4$ eV and disperses upward in energy to $E_F + 1.4$ eV at $\bar{M}$. Near $\bar{M}$ the band is primarily of $d_{x^2-y^2}$ character and has been identified in all three slab calculations [17, 18, 21]. The third experimental band is thus in fair agreement with a combination of our SS/SR bands. Along $\bar{\Delta}$ the agreement is with the calculated bands which terminate at $E_F - 1.6$ eV at $\bar{\Gamma}$ and at $E_F - 3.2$ eV at $\bar{X}$. Along $\bar{\Sigma}$ the experimental band is close to the higher energy $\bar{\Sigma}_2$ surface state band, having a minimum in the middle of $\bar{\Sigma}$ at the same energy, $E_F - 2.4$ eV, as

that calculated. The experimental band continues on to $E_F - 1.5$ eV at $\bar{\Gamma}$, which agrees well with our $\bar{\Gamma}$ surface resonance energy.

The fourth occupied $\bar{\Gamma}$ peak is located at $E_F - 0.3$ eV. It has $\Delta_{2'}$ symmetry (Δ_2 with respect to bulk axes), and is composed of d_{xy} states. It lies near the top, but within, the bulk Δ_2 band; thus is a surface resonance. Along $\bar{\Delta}$ the band has $\bar{\Delta}_2$ (odd) symmetry and persists to about one-third of the way to $\bar{X}$, dispersing downward in energy. Along $\bar{\Sigma}$ the band has even ($\bar{\Sigma}_1$) symmetry and disperses downward in energy as a SR to one-third of the way to $\bar{M}$. The band then enters the even-symmetry hybridization gap and extends past halfway to $\bar{M}$ as a SS band. The same band is seen on Ir(001) beginning just above E_F [21]. This band may also be seen in the 5-layer calculation; however, there the band is unoccupied at $\bar{\Gamma}$ and disappears along $\bar{\Delta}$ all the way to $\bar{X}$. The first third of the fourth experimental band agrees well in positioning and dispersion with our $\bar{\Delta}_2$ band which starts at $\bar{\Gamma}$, $E_F - 0.3$ eV. However, there is no agreement with any theoretical band for the latter two-thirds of $\bar{\Delta}$. Along $\bar{\Sigma}$ there is again good agreement with theory near $\bar{\Gamma}$, but no agreement beyond one-eighth $\bar{\Sigma}$.

Several other calculated bands are worthy of note. A very intense $\bar{X}$ surface resonance peak of d_{xz} and d_{yz} character is observed at $E_F - 2.5$ eV. About 0.6 eV higher in energy a small band of $\bar{\Delta}_2$ surface states can be identified in the $\bar{\Delta}_2$ symmetry gap near $\bar{X}$. From the midpoint of $\bar{\Delta}$ at $E_F - 2.9$ eV, dispersing toward the zone boundary and terminating in an $\bar{X}$ state at $E_F - 0.2$ eV, is a surface state band of $\bar{\Delta}_1$ symmetry. This is a true surface state band because it exists in the large $\bar{\Delta}_1$ relative gap. The same band has been observed in both the 5-layer Pt(001) and 14-layer Ir(001) slab calculations [17, 21]. Although the band consists of a combination of d_{xz}, $d_{x^2-y^2}$, and d_{z^2} states, closer to $\bar{X}$ the SS is of primarily d_{xz} character. There is no experimental evidence of this $\bar{\Delta}_1$ surface state band, despite its existence in all three calculations.

Above the Fermi level there are $\bar{\Gamma}$ surface state peaks at $E_F + 0.3$ eV and $E_F + 1.2$ eV. The first is a Tamm state pulled off the top of the bulk Δ_2 band. Along $\bar{\Delta}$ the band rapidly hybridizes with the odd symmetry ($\bar{\Delta}_2$) bands. The higher energy peak is also a Tamm state, pulled from the bulk Δ_5 band. It is composed predominantly of $d_{xz,yz}$ states, and is the antibonding partner of the surface resonance at $E_F - 1.6$ eV.

Two additional experimental bands are not observed in our theoretical electronic structure. A band is observed at $E_F - 2.3$ eV near $\bar{M}$. In addition, there are experimental peaks observed between $E_F - 7$ eV and $E_F - 8$ eV in the middle half of $\bar{\Sigma}$. From our projected band structure, these peaks appear to be located below the bottom of the bulk valence band.

As previously mentioned, valence states were computed scalar-relativistically (the spin–orbit term omitted), while core states were calculated fully relativistically. As is well known, the spin–orbit (S-O) term has a negligible effect on the bandstructure of lighter elements; however, for heavier elements it becomes increasingly important. For the 5d transition series the splitting of degenerate states is of the order of 1 eV [22, 29]—the splittings being mainly between the $d_{3/2}$ and $d_{5/2}$ portions of the band. In the case of platinum, however, the inclusion of the spin–orbit interaction does not greatly alter the self-consistent potential. This is because the more $d_{3/2}$-like and $d_{5/2}$-like parts of the d band lie well below the Fermi energy. Consequently the d-band filling is little changed, and reasonable work functions may be obtained from scalar-relativistic calculations. Below E_F the semirelativistic wavefunctions approximately average the S-O split portions of the band [22].

Bertoni *et al* [30] have compared the projected bulk band structures obtained from relativistic and nonrelativistic calculations for Ir(001). Gaps near the Fermi level are

hardly modified. The only significant changes occur for gaps near $E_F - 4$ eV. As discussed above, a spin–orbit gap is opened up across the entire surface Brillouin zone centred approximately on $E_F - 4$ eV. It is believed that the band observed along both $\bar{\Delta}$ and $\bar{\Sigma}$ in the angle-resolved photoemission data is a surface state band in this gap.

3.3. Reconstruction

The (001) surface of platinum is also of interest because of the (5 × 20) reconstruction it exhibits. An early photoemission experiment revealed that a prominent surface peak just below E_F was dramatically attenuated upon reconstruction. Bonzel *et al* [9] suggested that the rehybridization or splitting of the peak could lower the surface energy and drive the reconstruction.

The various contributions to the electronic pressure in transition and noble metals have been discussed by Christensen and Heine [31] and Heine and Marks [32]. In the middle of the transition series the attractive d electron interaction attempts to compress the bond lengths. This compression is resisted by the sp electrons whose kinetic energy rises with the decrease in atomic volume. As one approaches the noble metal end of the transition series, however, this picture alters considerably. As the antibonding states at the top of the d-band fill, the attractive interaction between the d orbitals first diminishes, and then changes sign as the interaction becomes of the closed shell (repulsive) type. In addition, a multi-atom attractive interaction arises due to the sp electrons and the sp–d hybridization. The origin of this interaction is due to an anomalously attractive region just inside the core of the noble metals. The attractive region is the result of an incomplete cancellation between the outermost s and d core orbitals due to their different radii. Experimental support for this point of view comes from the alloy work of Nevitt [33]. He found that the apparent atomic volume of Cu, Ag and Au was reduced when alloyed with metals with small atomic cores. With the d bands no longer in 'contact' the repulsion is diminished and the attractive sp interactions reduce the atomic volumes. The volume reductions were considerable—amounting to over 20% of the atomic Au volume in CsCl-type compounds [33].

It is interesting that the same volume reduction observed in the noble metals is also seen in compounds containing Pd [33]. Pettifor takes the crossover to repulsive d–d and attractive sp interactions in the 4d transition series to be at Pd [34]. Both Pd in the 4d series and Pt in the 5d series have all of their d-states occupied as free atoms. In the solid, part of the d band lies above the Fermi energy due to hybridization; however, the d band is nearly full, and one would still expect the d–d interaction to be repulsive. Since the effects are stronger in the 5d series, it is likely that Pt, too, should be classified along with the noble metals. This is consistent with calculated surface stresses in the 5d series which indicate larger compressive surface stresses for Ir and Pt (which have fewer d electrons) than for Au [35].

Recently, Annett and Inglesfield have estimated the enhancement of surface bonds on Au(001) by analyzing the surface charge density [36]. Using a tight-binding expression for the Hellmann–Feynman force between two atoms, they concluded that the balance between repulsive d and attractive sp–d and sp forces was broken at the surface because of an increase in sp bonding charge.

Following Annett and Inglesfield [36], we overlapped atomic charge densities for neutral Pt atoms to find a mid-bond charge density of 0.0487 $Å^{-3}$. A superposition of Pt^+ ions produces a mid-bond charge density of 0.0348 $Å^{-3}$. We take these to be the non-bonding and d-only contributions to the total charge density. Our self-consistent

charge density for the surface layer yields a mid-bond density of 0.0581 $Å^{-3}$. For the mid-bond density in the bulk we use the value of 0.055 $Å^{-3}$ from Weinert and Freeman's [18] slab calculation.

The bond order B for identical s states $\varphi(r)$ with half-occupancy on atoms i and j is given by:

$$\rho_b = (2B + 2)|\varphi(R_{ij}/2)|^2$$

where ρ_b is the charge density at the mid-point of the bond. Using the listed charge densities we calculate a surface sp bond order of 0.7 compared with a bulk bond order of about 0.45. The surface enhancement of the bond order in Pt is very close to that found for Au.

The sp contribution to the Hellmann–Feynman force between the two atoms can be computed from the tight-binding expression:

$$F_{ij} = -2B\,\partial H/\partial R_{ij}$$

where H is the matrix element of the Hamiltonian between the two orbitals.

Annett and Inglesfield obtain an estimate for $\partial H/\partial R_{ij}$ from the d–d repulsion at equilibrium calculated in [32]. The Pt lattice constant of 3.92 Å is about 4% smaller than that of Au. This contraction is consistent with a reduced d–d repulsion at the Au lattice constant due to the removal of about half of a d electron. However, as in Au, the sp contractive pressure rises as the lattice constant diminishes near equilibrium; so that when equilibrium is re-established at the smaller lattice constant, it is between pressures that are larger in magnitude. Estimating the increased pressure from the calculated values for Au, a 4% contraction in the lattice constant leads to an increase in s and p pressure of about 70 kbar or a total contractive pressure of 200 kbar at the Pt equilibrium distance [32]. Dividing the pressure among the nearest neighbour bonds yields an attractive bonding force F_s of 0.31 eV $Å^{-1}$. At the surface, the sp bonds are strengthened by a factor equal to the ratio of the surface to bulk bond orders. Assuming that the d–d and s–d hybridization remain the same at the surface as in the bulk, the net compressive force per bond becomes $F = (0.7/0.45 - 1)\,F_s = 0.17$ eV $Å^{-1}$. The surface stress g is equal to the ratio F/d, where d is the interatomic spacing, 2.77 Å. If both of the top two atomic layers have the same enhancement, as is the case for Au(001), then the total surface stress is 0.12 eV $Å^{-2}$—slightly higher than that obtained for Au(001). The surface stress on the (111) face is expected to be $\sqrt{3}\,F/d$, assuming the same bond enhancements. This gives a (111) surface stress of 0.21 eV $Å^{-2}$. This value is larger than the experimental surface energy of 0.159 eV $Å^{-2}$ [37], but is not as large as the calculated surface stress of 0.350 eV $Å^{-2}$ [35]. The agreement is reasonable considering the simplicity of the model we have used. Agreement should be improved by including the effect of changes in s–d hybridization at the surface; which, with the upward shift in potential at the surface, could be expected to put more antibonding d-weight above E_F and lead to an increased surface stress.

Thus, our calculated charge density indicates an increased sp bonding charge which dominates the d–d repulsive interaction, and leads to a compressive surface stress. The high value of the surface stress is consistent with the reconstruction of the (1 × 1) Pt(001) surface to the (5 × 20) phase. While other factors, such as the energy cost of altering the density of atoms in the surface layer and the effect of the surface-subsurface interactions, must be taken into account [35], it is evident that a high surface stress destabilizes the surface layer(s) and may lead to the observed reconstruction.

4. Conclusions

The metastable (1 × 1) Pt(001) surface has been studied with the goal of identifying those surface state/surface resonance bands which, together with the molecular orbitals of the chemisorbed species, determine the crystal face-dependent catalytic activity. Unlike slab calculations, we have included the bulk energy bands directly in the calculation via the embedding potential, so that the positioning and dispersion of SS/SR resonance bands may be accurately determined. The agreement with angle-resolved photoemission experiments for the metastable surface is good, although there remain some unresolved features—primarily near E_F. Our results help clarify the understanding of states found experimentally and in earlier slab calculations.

The calculated total charge density is similar to that of both 5-layer slab LAPW calculations. The resulting work function of 5.92 ± 0.09 eV is in excellent agreement with experiment and gives us confidence that the charge density has been accurately determined. An analysis of the distribution of charge at the surface yielded an increase in the sp bonding charge. It was shown how the increased sp charge unbalances the pressures present at the surface, and leads to a compressive surface tension.

Acknowledgments

The authors are grateful to D A King for making unpublished photoemission data available, to M Weinert for supplying a bulk platinum potential, to R J Needs for helpful discussions, and to J A Sams for computational assistance. We gratefully acknowledge financial support from The Robert A Welch Foundation (grant number AA-1033) and from the Science and Engineering Research Council (grant number GR/F95696).

References

[1] Bonzel H P and Fisher T E 1975 *Surf. Sci.* **51** 213
[2] Nieuwenhuys B E 1983 *Surf. Sci.* **126** 307
[3] Behm R J, Thiel A, Norton R and Ertl G 1983 *J. Chem. Phys.* **78** 7437
[4] Somorjai G A 1983 *Proc. of the Robert A Welch Foundation: Conf. on Chemical Research, XXV. Heterogeneous Catalysis* (Houston, TX: Robert A. Welch Foundation) pp 83–140
[5] Loeffler D G and Schmidt L D 1976 *Surf. Sci.* **59** 195
[6] Adzic R R, O'Grady W E and Srinivasan S 1980 *Surf. Sci.* **94** L191
[7] Banholzer W F, Gohndrone J M, Hatzikos G H, Lang J F, Masel R I, Park Y O and Stolt K 1985 *J. Vac. Sci. Technol.* A **3** 1559
[8] Brooks R S and King D A to be published
Brooks R S 1985 *PhD Thesis* Cambridge University
[9] Bonzel H P, Helms C R and Kelemen S 1975 *Phys. Rev. Lett.* **35** 1237
[10] Benesh G A and Inglesfield J E 1984 *J. Phys. C: Solid State Phys.* **17** 1595
[11] Inglesfield J E and Benesh G A 1988 *Phys. Rev.* B **37** 6682
[12] Weinert M private communication (Brookhaven National Laboratory)
[13] Hedin L and Lundqvist B I 1971 *J. Phys. C: Solid State Phys.* **4** 2064
[14] Cunningham S L 1974 *Phys. Rev.* B **10** 4988
[15] Mundschau M and Vanselow R 1985 *Surf. Sci.* **157** 87
[16] Drube R, Dose V and Goldmann A 1988 *Surf. Sci.* **197** 317
[17] Wang D S, Freeman A J and Krakauer H 1984 *Phys. Rev.* B **29** 1665
[18] Weinert M and Freeman A J 1983 *Phys. Rev.* B **28** 6262
[19] Benesh G A and Inglesfield J E 1986 *J. Phys. C: Solid State Phys.* **19** L539
[20] Inglesfield J E and Benesh G A 1988 *Surf. Sci.* **200** 135

[21] Bisi O, Calandra C and Manghi F 1977 *Solid State Commun.* **23** 249
[22] MacDonald A H, Daams J M, Vosko S H and Koelling D D 1981 *Phys. Rev.* B **23** 6377
[23] Pirug G, Bonzel H P, Hopster H and Ibach H 1979 *J. Chem. Phys.* **71** 593
[24] Gurman S J and Pendry J B 1973 *Phys. Rev. Lett.* **31** 637
[25] Sohn K S, Dempsey D G, Kleinman L and Caruthers E 1976 *Phys. Rev.* B **13** 1515
[26] Arlinghaus F J, Gay J G and Smith J R 1980 *Phys. Rev.* B **21** 2055
[27] Gay J G, Smith J R, Arlinghaus F J and Capehart T W 1981 *Phys. Rev.* B **23** 1559
[28] Pick Š and Tomášek M 1978 *Czech. J. Phys.* B **28** 781
[29] Andersen O K 1970 *Phys. Rev.* B **4** 883
[30] Bertoni C M, Bisi O, Calandra C and Manghi F 1978 *Transition Metals 1977* (*Inst. Phys. Conf. Ser. 39*) ed M J G Lee, J M Perz and E Fawcett (Bristol: Institute of Physics) p 329
[31] Christensen N E and Heine V 1985 *Phys. Rev.* B **32** 6145
[32] Heine V and Marks L D 1986 *Surf. Sci.* **165** 65
[33] Nevitt M V 1967 *Physe Stability of Metals and Alloys* ed P S Rudman, J Stringer and R I Jaffee (New York: McGraw-Hill) pp 281–90
[34] Pettifor D G 1978 *J. Phys. F: Met. Phys.* **8** 219
[35] Needs R J and Mansfield M 1989 *J. Phys: Condens. Matter* **1** 7555
[36] Annett J F and Inglesfield J E 1989 *J. Phys: Condens. Matter* **1** 3645
[37] Miedema A R 1978 *Philips Tech. Rev.* **38** 257